J Neurophysiol
88: 2311–2321, 2002; 10.1152/jn.00372.2002.

Segregation of ON and OFF Retinogeniculate Connectivity Directed by Patterned Spontaneous Activity

CHRISTOPHER W. LEE, STEPHEN J. EGLEN, AND RACHEL O. L. WONG
Department of Anatomy and Neurobiology, Washington University School of Medicine, St. Louis, Missouri 63110

Received 16 May 2002; accepted in final form 6 August 2002

Lee, Christopher W., Stephen J. Eglen, and Rachel O. L. Wong. Segregation of ON and OFF retinogeniculate connectivity directed by patterned spontaneous activity. *J Neurophysiol* 88: 2311–2321, 2002; 10.1152/jn.00372.2002. In many parts of the developing nervous system, the early patterns of connectivity are refined by processes that require neuronal activity. These processes are thought to involve Hebbian mechanisms that lead to strengthening and maintenance of inputs that display correlated pre- and postsynaptic activity and elimination of inputs that fire asynchronously. Here we investigated the role of patterned spontaneous retinal activity and Hebbian synaptic mechanisms on segregation of ON and OFF retinal afferents in the dorsal lateral geniculate nucleus (dLGN) of the developing ferret visual system. We recorded extracellularly the spontaneous spike activity of neighboring pairs of ganglion cells and found that OFF cells have significantly higher mean firing rates than ON cells. Spiking is best correlated between cells of the same sign (ON, ON; OFF, OFF) compared with cells of opposite sign (ON, OFF). We then constructed a simple Hebbian model of retinogeniculate synaptic development based on a correlational framework. Using our recorded activity patterns, together with previous calcium-imaging data, we show that endogenous retinal activity, coupled with Hebbian mechanisms of synaptic development, can drive the segregation of ON and OFF retinal inputs to the dLGN. Segregation occurs robustly when heterosynaptic competition is present within time windows of 50–500 ms. In addition, our results suggest that the initial patterns of connectivity (biases in convergence of inputs) and the strength of inhibition in the network each play a crucial role in determining whether ON or OFF inputs dominate at maturity.

INTRODUCTION

The early patterns of connectivity in the central and peripheral nervous systems are imprecise. As development proceeds, appropriate synaptic inputs are strengthened and maintained, whereas inappropriate connections are weakened and eliminated. Much evidence suggests that neuronal activity plays a key role in the refinement process, but how activity mediates synapse rearrangement is not yet fully understood (Goodman and Shatz 1993; Sanes and Lichtman 1999). It is apparent, however, that neurotransmission per se is insufficient, but rather the relevant information is likely to be encoded in the temporal organization of the spike patterns and in the coordinated activity of pre- and postsynaptic cells (Eglen 1999; Goodhill and Löwel 1995; Miller 1996; Stryker and Strickland 1984).

To understand how patterned spike activity shapes connectivity, many theoretical approaches have represented neuronal activity in mathematically convenient, idealized forms that may not correspond to biologically generated activity patterns (Linsker 1986; Miller et al. 1989; reviewed in van Ooyen 2001). This is because few measurements on the endogenous patterns of activity in the developing nervous system have been possible. In this study, we measured the patterns of activity in the developing ferret visual system that have been hypothesized to refine connectivity (Goodman and Shatz 1993; Wong 1999). We then examined whether these patterns provide cues for the observed in vivo changes in connectivity.

In the ferret visual system, functionally distinct ON- and OFF-center retinal ganglion cells (RGCs) connect to separate neurons in their central target, the dorsal lateral geniculate nucleus (LGN), at maturity (Zahs and Stryker 1988). However, ON and OFF axonal terminals overlap in the LGN early in development. Because ON and OFF projection patterns refine prior to vision and require retinal spike activity (Cramer and Sur 1997; Hahm et al. 1991), spontaneous activity from the retina is thought to provide the cues necessary for this refinement process. But, as yet, it is not well understood whether the spike patterns of the ON and OFF cells contain information required to drive segregation of their axonal projections.

Previously, using calcium imaging, morphologically identified ON and OFF RGCs demonstrate different activity patterns during the period when their axonal terminals segregate in the LGN (Wong and Oakley 1996). However, the calcium-activity patterns do not necessarily provide information about the spike patterns of the RGCs. We thus recorded extracellularly from pairs of morphologically identified ON or OFF RGCs to determine the temporal correlations of the firing of these cells. We then explored what information may be provided by their spiking patterns that could lead to the segregation of their connectivity with geniculate neurons under a simple, linear Hebbian rule (Hebb 1949).

METHODS

Tissue preparation

Ferrets aged between postnatal days (P) 16 and 24 were obtained from Marshall Farms. The animals were killed by 5% halothane inhalation followed by decapitation. The eyes were enucleated and the

Address for reprint requests: R.O.L. Wong, Department of Anatomy and Neurobiology, Washington University School of Medicine, 660 S. Euclid, St. Louis, Missouri 63110 (E-mail: wongr@thalamus.wustl.edu).

The costs of publication of this article were defrayed in part by the payment of page charges. The article must therefore be hereby marked "*advertisement*" in accordance with 18 U.S.C. Section 1734 solely to indicate this fact.

retinas dissected in cold (4°C) oxygenated Ames medium (Sigma, St. Louis, MO). Each retina was hemisected, mounted on a glass slide, and held flat by a piece of black Millipore filter paper. A hole (approximately 3×3 mm^2) in the filter paper allowed visualization of the cells in the ganglion cell layer under Normarski optics. The retinas were maintained in a recording chamber at 35°C in oxygenated Ames medium. A total of 21 animals and 32 retinas were used; spike trains were analyzed from six ON-ON, six OFF-OFF, and 15 ON-OFF cell pairs. Intracellular calcium imaging data obtained from a previous study (Wong and Oakley 1996) was also used for this study.

Spike recordings and analysis

Extracellular electrodes were pulled from borosilicate glass (0.94 mm ID, 1.2 mm OD; Sutter Instruments, Novato, CA, BF120-94-10). To obtain resistances of approximately 5 MΩ and to ease penetration through tissue, the electrodes were then beveled at approximately 30° (Sutter Instruments). The electrodes were filled with Ames medium. Spikes were acquired using an Axopatch 200B and an AM Systems 1200 amplifier with the signals stored on digital audio tape (Dagan, Minneapolis, MN, DAS-75/Sony DAT model DTC-ZE700). Signals were band-pass filtered between 300 and 2,000 Hz and re-sampled at 8 kHz for analysis. At these stages of development, alpha RGCs produce stereotyped patterns of high-frequency firing (200–500 Hz), lasting 5–10 ms (Wong et al. 1993) (Fig. 1*A*). Resolving each action potential within such a rapid spike burst is known to be an unsolved problem in spike sorting (Lewicki 1998). Therefore for the purposes of simulations and analysis, each rapid spike burst was counted as a single event or "complex action potential" based on the close resemblance between our phenomenon and the complex spikes seen in cerebellar Purkinje cells. Spike timings were obtained using custom software to match the templates of alpha cell complex spikes. Because our linear correlational model is invariant to global scaling factors, this method of counting of alpha cell action potentials does not affect the conclusions based on our analysis but would affect comparisons with other RGC types, e.g., beta cells. Statistical tests were performed using R, an open source implementation of the S statistical language (http://www.r-project.org).

Statistical measures of cell firing

Statistical measures for mean cell firing rates and pair correlation coefficients were calculated using standard definitions. Measures of correlation depend on the size of the time window, Δt, over which activity in the two cells of a pair are considered coincident. Given a time window Δt, each cell spike train was divided into M bins of size Δt to produce an array, $N_{\Delta t}(t_m)$, which measured the number of spikes in the mth bin. This was converted into a measure of the firing rate, $r_{\Delta t}(t_m)$, of the cell over time as defined by

$$r_{\Delta t}(t_m) = \frac{N_{\Delta t}(t_m)}{\Delta t} \quad (1)$$

Correlation coefficients, $\rho_{\Delta t}(r_1,r_2)$, between cells with firing rates, $r_{1,\Delta t}(t_m)$ and $r_{2,\Delta t}(t_m)$ are given by

$$\rho_{\Delta t}(r_1, r_2) = \frac{\mathrm{Var}_{\Delta t}(r_1, r_2)}{\sqrt{\mathrm{Var}_{\Delta t}(r_1, r_1)\mathrm{Var}_{\Delta t}(r_2, r_2)}} \quad (2)$$

where the variance operator, $\mathrm{var}_{\Delta t}(r_j,r_k)$, is defined by

$$\mathrm{Var}_{\Delta t}(r_j, r_k) = \frac{1}{M-1}\sum_{m=1}^{M}(r_{j,\Delta t}(t_m) - \overline{r_{j,\Delta t}})(r_{k,\Delta t}(t_m) - \overline{r_{k,\Delta t}}) \quad (3)$$

For a given Δt, we also calculated a related statistic, the raw cross-correlation between a pair of cells, i and j, as

$$C_{ij} = \frac{1}{M}\sum_{m=1}^{M} r_{i,\Delta t}(t_m) r_{j,\Delta t}(t_m) \quad (4)$$

The correlation matrix is then formed from these cross-correlations, which is then used to determine whether the inputs segregate (Mackay and Miller 1990).

Identification of ON and OFF cells

Two major classes of RGCs form ON and OFF subtypes, alpha and beta cells (Wässle and Boycott 1991). We focused on alpha RGCs in this study for several reasons. First, alpha cells are easier to identify and target due to their relatively large size. Second, they are spaced relatively far apart compared with beta cells, thus enabling us to more easily separate the spikes from pairs of cells recorded simultaneously. Third, alpha cells have characteristic spike patterns—in contrast to beta cells which generate a single spike per depolarization, alpha cells fire in doublets or multiplets of spikes (Fig. 1*A*). This latter spike

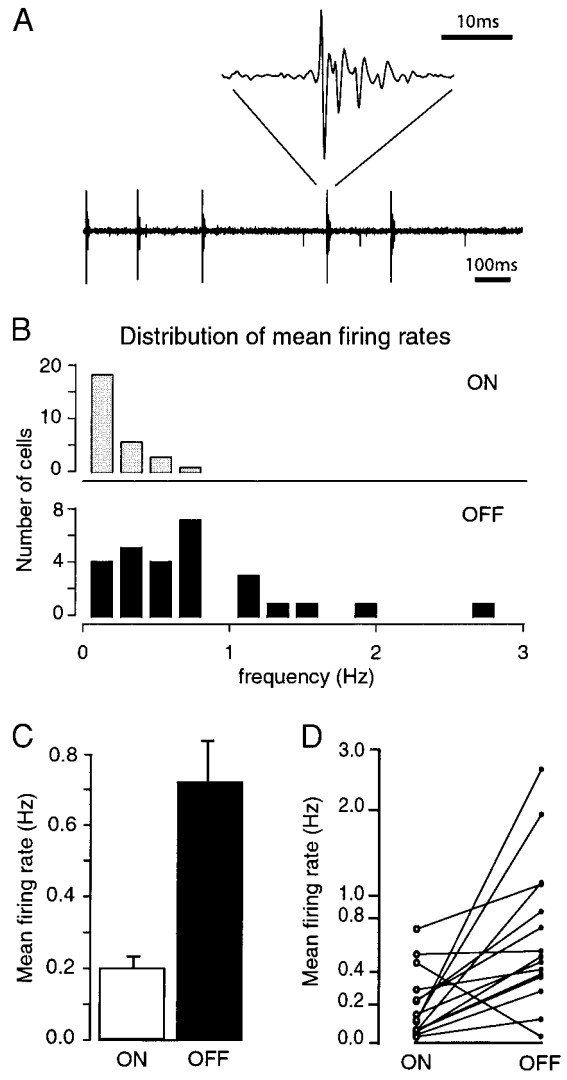

FIG. 1. Spike patterns of ON and OFF retinal ganglion cells (RGCs). *A*: extracellular recording of the spike patterns of a P18 ON alpha RGC. An expanded view (*top*) of the spikes showing a multiplet, or "complex spike," that is characteristic of these cells. *B*: the distribution of mean firing rates for ON and OFF cells. *C*: mean firing rates for the ON and OFF cell populations. OFF cells fired at significantly higher rates (t-test: $P < 0.01$). *D*: mean firing rates for pairs of ON and OFF cells recorded simultaneously.

feature of alpha cells allowed us to confidently associate the spike trains to a given cell.

After recording, an intracellular electrode filled with Lucifer yellow (4% in 0.1 M LiCl) was used to target and dye-fill the recorded cell. In the ferret retina, presumed ON and OFF types of alpha cells can be identified based on their dendritic stratification levels after the first postnatal week (Bodnarenko et al. 1999; Lohmann and Wong 2001). ON cells have dendritic arbors that terminate within the inner half of the inner plexiform layer (IPL), whereas OFF cells stratify in the outer half of the IPL. The dendritic stratification level of each cell was obtained by focusing through the IPL and determining the distance of the terminal dendrites from the boundaries of the IPL. Under Normarski optics, the boundaries of the IPL can be viewed; the inner boundary begins at the base of the RGC body and the outer boundary is located at the inner nuclear layer/IPL interface. When viewed together with the fluorescence from the dye-filled cells, it is possible to register the dendritic stratification levels of the cell with the IPL boundaries. This method of determining the stratification levels of the dye-filled cells has been used successfully in previous recordings both in developing and more mature ferret retinas (Lohmann and Wong 2001; Myhr et al. 2001; Wong and Oakley 1996).

Mathematical and computational methods

LINEAR CORRELATION-BASED MODEL FOR SYNAPTIC DEVELOPMENT. For our analysis, we use a simple mathematical model based on a linear correlation-based form of synaptic plasticity (Linsker 1988; MacKay and Miller 1990; Miller 1994; Miller et al. 1989). Unlike models that attempt to represent the detailed biophysical mechanisms of the neuronal system (cf. Koch and Segev 1998), correlation-based systems are "reduced-parameter" models designed to capture a few essential features of synaptic modification that arises due to patterned pre- and postsynaptic activity. Mathematically, it can be derived from more biophysically accurate models (Miller 1990) and as such comprises a first- and second-order approximation to the biological system. It follows that linear correlational models occupy an important position among parameterized models because they represent the simplest systems that capture the effects on synaptic development of differences in both the mean firing rates and the correlated firing patterns of cells.

We begin defining our model by schematizing the elements of the retinogeniculate network. We simplify the system to a set of RGCs that make excitatory synaptic contact with a given dorsal lateral geniculate (dLGN) relay cell (see Fig. 2*A*). The activity of the relay cell is considered to be a function of its retinal inputs and any local inhibitory activity. Let x_j denote the presynaptic activity of the jth RGC. Let y denote the activity of the dLGN relay cell, and let I denote

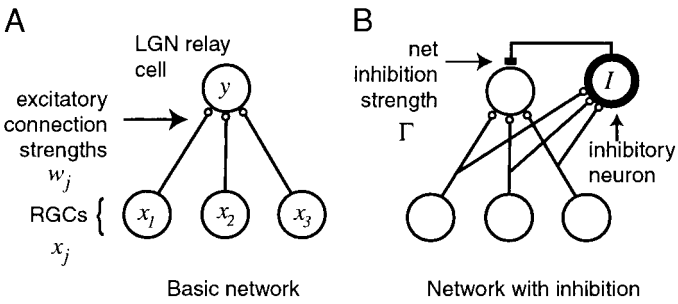

FIG. 2. Network architecture of the model. *A*: basic structure of the network. A group of RGCs, represented here by the 3 circles labeled with x_1, x_2, x_3, provide input to the lateral geniculate (dLGN) cell via excitatory synapses (small open circles) with strengths w_j where $j \in \{1,2,3\}$. At any given moment, the dLGN cell's activity is represented by y. *B*: the full network architecture, including an inhibitory component. The inhibitory cell or group of cells (labeled by I at top right) receives a net excitatory input as a result of RGC activity. Net inhibition onto the dLGN cell is given by Γ.

the net presynaptic inhibitory activity. The strength of the connection between the jth RGC and the postsynaptic cell is denoted by a synaptic weight, $w_j \in [0,1]$, where a value of 1 represents a maximally strong connection.

The general equation for how the synaptic weight w_j changes per unit time, Δt, is of the form

$$\Delta w_j = F(y, x_1, x_2, \ldots, x_j, \ldots, x_N, I, t) \quad (5)$$

in which F stands in for some appropriate function of its inputs. We will consider the dLGN postsynaptic activity as a linear weighted sum of its excitatory and inhibitory inputs. We will also consider a simplified form of dLGN inhibitory network (illustrated in Fig. 2*B*). A single inhibitory cell with activity I is posited to receive inputs from the RGCs with synaptic strengths γ_j. This cell in turn makes a synapse on the dLGN relay cell via a synapse with strength γ'. By assuming that all inhibitory synapses are equal, the gamma parameters (γ_j and γ') can be combined into a single parameter, Γ, a real-valued number between zero and one that summarizes the overall level of inhibition in the system. It is also assumed that synaptic strengths change slowly relative to the rate of bursts. To enforce this assumption, we therefore insert a small-valued parameter, η, as a proportionality constant. (Together, these assumptions greatly reduce the potential complexity of *Eq. 5*). Finally, we add another parameter θ ($\theta \geq 0.0$ Hz), which sets the levels of an inter-synaptic interaction to induce synaptic competition (further explanations in the following text).

Incorporating the assumptions from the preceding text, *Eq 5.* becomes

$$\Delta w_j = \eta y(x_j - \theta) \quad (6)$$

with inhibition defined by

$$I = \sum_j \gamma_j x_j = \Gamma \sum_j x_j \quad (7)$$

Given that we assume that the postsynaptic activity, y, is a weighted sum of its inputs and given the assumptions on the gamma parameters mentioned in the preceding text, we produce a definition for the total postsynaptic activity

$$y = \sum_j w_j x_j - \Gamma \sum_j x_j \quad (8)$$

The relationship between linear Hebbian learning and correlation is seen by substituting *Eq. 8* into *Eq. 6* and rearranging giving

$$\Delta w_i = \eta \sum_j (x_j x_i - x_j \theta)(w_j - \Gamma) \quad (9)$$

Averaging over the ensemble of the set of $\{x_i\}$ and assuming that the x_i's change more quickly than the w_i's, then

$$\Delta w_i \approx \langle \Delta w_i \rangle = \eta \sum_j (C_{ij} - \bar{x}_j \theta)(w_j - \Gamma) \quad (10)$$

where C_{ij} is the correlation matrix of the input activities, $C_{ij} = \langle x_i x_j \rangle$, and $\bar{x}_j$ is the mean value of each x_j (angled brackets, $\langle \ldots \rangle$, indicate the averaging operation). This emphasizes the dependence synaptic growth has on correlations (C_{ij}) and mean levels ($\bar{x}_i$) of input activity.

It is clear from *Eq. 9* that development of connections in the model are affected by four major factors: the pattern of input activity, the initial connectivity, the parameter θ, and the parameter Γ. The pattern of input activity and the initial connectivity have clear biological equivalents, but what is the significance of the parameters θ and Γ? As noted in the preceding text, Γ represents the total level of inhibition on the dLGN cell and acts to balance the excitatory drive from the retina to the dLGN relay cell. This parameter could therefore correspond to the inhibitory network in the dLGN that is developing during the period of ON-OFF segregation. On the other hand, θ, the "level of heterosynaptic competition" can be understood in terms of mecha-

nisms that induce competition between synaptic inputs. As θ increases from 0 Hz, it increases the punishment inactive synapses receive when active synapses grow and vice versa. For example, if an input, x_j, remains zero while y is positive, the synapse w_j will be decremented by an amount proportional to θ. We will examine the effect of changes in both the level of inhibition, Γ, and the "competition parameter," θ in the following text.

ANALYSIS AND SIMULATIONS. Both analytical (Hertz et al. 1991; Mackay and Miller 1990) and simulation techniques were used to determine the outcome of the model under different conditions. For the spike data, the eigenvectors and eigenvalues of the correlation matrix were computed using Mathematica (Wolfram 1999) and LAPACK (Anderson et al. 1995) to test whether the two inputs would segregate. This analysis was verified by simulation. For the calcium-imaging data, computer simulations were performed via the finite difference version of *Eq. 9*. The step size, $\eta = 0.001\ \mathrm{Hz}^{-2}$, was chosen to ensure that the slow-growth-per-burst assumption used in the analysis was met. Experimental data were used as input by inserting the values of spike rates or calcium activity as a stream of inputs with cyclic repetition of the input. Unbiased initial connection strengths were chosen uniformly in the range [0.45,0.55] using pseudo-random number generation. Computer simulations were run typically for 10^6 iterations. At the end of each run, SIGN and DSEG (defined in the next section) were calculated to determine whether segregation of inputs had occurred.

QUANTITATION OF SEGREGATION. When dLGN cells received more than two inputs, the degree of dominance of an dLGN cell by either ON or OFF afferents was quantified by two measures, "SIGN" and "DSEG". SIGN is defined for each dLGN cell and varies from complete OFF dominance with SIGN = −1 to complete ON dominance with SIGN = 1 as defined by

$$\mathrm{SIGN} = \frac{(\text{Response to ON}) - (\text{Response to OFF})}{(\text{Response to ON}) + (\text{Response to OFF})} \qquad (11)$$

where the response to ON (or OFF) is the activity of the dLGN cell when all of the ON (or OFF) inputs are set to one. To measure a dLGN cell's degree of input segregation irrespective of the sign of the inputs, the absolute value of SIGN was used. This measure is defined by

$$\mathrm{DSEG} = |\mathrm{SIGN}| \qquad (12)$$

and varies from 0 to 1 as the degree of segregation increases with a value of 1 indicating that the dLGN cell receives all of its input from either ON or OFF RGCs.

RESULTS

Spike patterns of ON and OFF RGCs

Figure 1*A* shows a typical example of the spike train recorded from an ON alpha RGC. The distributions of mean firing rates across the recorded populations of ON and OFF cells are summarized in Fig. 1*B*. Although there is overlap in the mean firing rates of ON and OFF cells, overall, OFF cells fired 3.5 times more often than ON cells. Because mean firing rates vary somewhat with retinal location and from one animal to another, we compared the mean firing rates of ON and OFF cells that were simultaneously recorded within a single field of view. Figure 1*D* shows that for 13 of 15 cell pairs, the OFF cell fired at a higher rate than the ON cell.

Temporal relationship between ON and OFF spiking activity

We next compared the spike relationships of simultaneously recorded pairs of RGCs of different combinations: OFF-OFF, ON-ON, and ON-OFF (Fig. 3). Despite the differences in firing rates, ON and OFF cells displayed a significant degree of positive correlation; bursts of spikes in the ON cells coincided temporally with spiking in nearby OFF cells, within a time scale of ±500 ms. The cross-correlograms for the cell pairs shown in Fig. 3 suggest that the correlations in spiking between same-sign pairs (ON-ON or OFF-OFF) may be higher than that of opposite sign pairs (ON-OFF). To determine if this was true for the recorded population, we computed (see METHODS) the pair correlation coefficients for the different combinations of cell pairs and for different time windows (Fig. 4). Our results show that for all time scales, the activities of same-signed pairs were

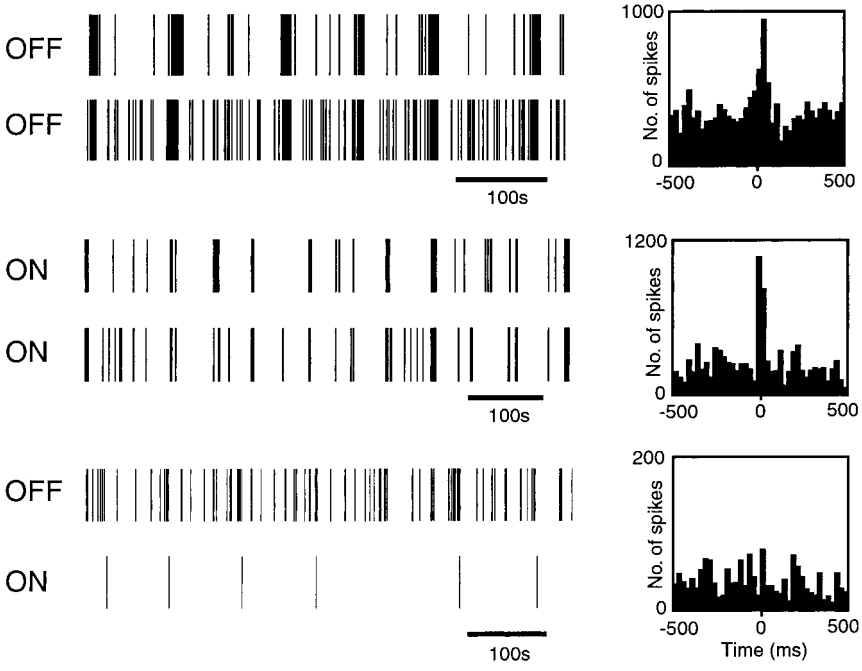

FIG. 3. Examples of spike activity of simultaneously recorded pairs of RGCs. Spike trains are rasterized. *Right*: cross-correlograms. Peaks of the correlograms near time $t = 0$ ms indicate that many spikes of both cells occurred within a time window of 25 ms (bin size) for the ON-ON and OFF-OFF cell pairs. The absence of a peak at or near $t = 0$ ms for the ON-OFF cell pair suggests that few spikes from this cell pair were correlated.

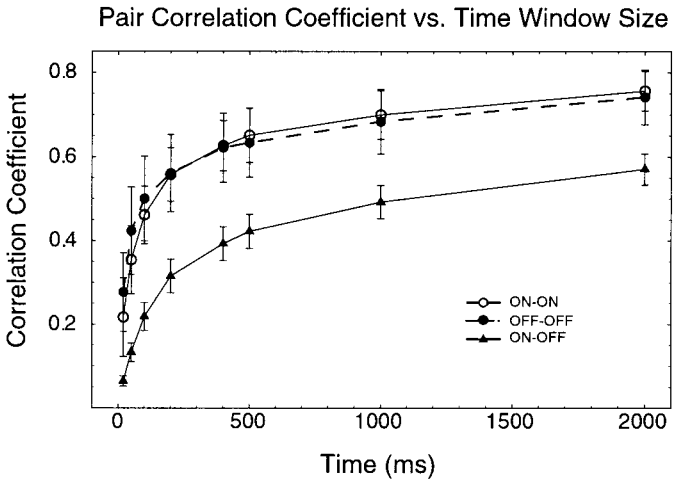

FIG. 4. Correlation coefficients of pairs of ON and OFF cells across different time windows. ON-ON and OFF-OFF pairs show higher correlation coefficients than ON-OFF pairs. The differences between same-signed pair coefficients and mixed-sign coefficients are statistically significant for all time scales from 50 to 2,000 ms (*t*-test: $P < 0.05$). Higher values of the correlation coefficient indicate that relatively more spikes of the same sign pairs occurred simultaneously within each time window. All coefficients are significantly above 0 (*t*-test: $P < 0.01$), indicating that the spike activity of all pairs, including those of opposite sign, are synchronized to some degree. This appears to be because each time an ON cell spikes, an OFF cell is also likely to spike.

significantly (*t*-test: $P < 0.05$) more correlated than that of opposite-signed pairs.

The mean input values, $\bar{x}_i$, and cross-correlation values, C_{ij}, for each cell pair are given in Table1 for $\Delta t = 50$ and 500 ms. For each cell pair, the correlations were stronger at 50 than 500 ms. These cross-correlations and mean input levels are reported here because they can be directly used in an eigensystem analysis to predict whether the two inputs will segregate (Hertz et al. 1991; Mackay and Miller 1990).

Temporal cues encoded in the activity patterns are relevant for ON-OFF segregation—model results

We can now ask if relative differences in synchrony can drive segregation of afferents within the context of our correlational model. As in our analysis of correlation in retinal spike trains, we chose time scales, Δt, of 50 or 500 ms for our model. For each pair, the spike recordings were converted into arrays of spiking rates using either 50 or 500 ms bin sizes and provided as input into simulations of our model. In this section, we first show results for a typical ON-OFF pair (Figs. 5 and 6) and then show results summarizing over all the cell pairs recorded (Fig. 7).

Figure 5*A* plots the synaptic evolution of a typical ON-OFF pair in the absence of competition and inhibition (i.e., $\theta = 0$ Hz and $\Gamma = 0$) with the ON and OFF cell synaptic weights w_{ON} and w_{OFF} each starting close to 0.5. The result is that both ON and OFF synaptic weights increase exponentially until they reach their maximum allowed values at 1.0. In contrast, Fig. 5*B* shows what happens when sufficient competition is present (e.g., $\theta = 4.0$ Hz and $\Gamma = 0.0$): the two synapses change in opposite directions as the OFF synapse strengthens and the ON synapse weakens. A similar result occurs in our third example (Fig. 5*C*), when both competition and inhibition are present (e.g., $\theta = 4.0$ Hz and $\Gamma = 0.7$). In this case, however, the ON connection strengthens and the OFF connection weakens. These

TABLE 1. *Mean input levels ($\bar{x}_i$) and cross-correlation matrix elements (C_{ij}) at $\Delta t = 50$, 500 ms for each cell pair*

			Δt = 50 ms			Δt = 500 ms		
Cell Pair (1–2)	$\bar{x}_1$	$\bar{x}_2$	C_{11}	C_{12}	C_{22}	C_{11}	C_{12}	C_{22}
ON-ON	0.10	0.04	0.10	0.01	0.04	0.28	0.05	0.09
ON-ON	0.14	0.24	0.14	0.14	0.27	0.53	0.78	1.65
ON-ON	0.16	0.19	0.16	0.06	0.21	0.34	0.21	0.40
ON-ON	0.18	0.17	0.19	0.04	0.18	0.75	0.42	0.65
ON-ON	0.20	0.11	0.26	0.04	0.11	1.07	0.37	0.38
ON-ON	0.30	0.19	0.33	0.07	0.19	1.11	0.62	0.69
ON-OFF	0.03	0.12	0.03	0.01	0.12	0.05	0.05	0.21
ON-OFF	0.05	0.51	0.05	0.02	0.65	0.09	0.12	1.26
ON-OFF	0.06	0.37	0.08	0.01	0.38	0.14	0.08	0.68
ON-OFF	0.06	1.12	0.06	0.01	1.78	0.08	0.12	3.82
ON-OFF	0.07	0.39	0.06	0.03	0.44	0.16	0.18	1.03
ON-OFF	0.11	1.94	0.13	0.02	2.37	0.20	0.21	3.57
ON-OFF	0.11	2.65	0.11	0.12	3.30	0.38	1.17	13.03
ON-OFF	0.15	0.48	0.14	0.06	0.58	0.44	0.65	1.87
ON-OFF	0.23	0.74	0.24	0.17	1.10	0.69	1.28	5.78
ON-OFF	0.28	0.04	0.39	0.01	0.04	0.74	0.10	0.07
ON-OFF	0.29	0.42	0.35	0.10	0.53	1.80	0.94	1.57
ON-OFF	0.46	0.03	0.83	0.02	0.04	3.62	0.20	0.07
ON-OFF	0.52	0.54	0.90	0.07	0.76	4.53	0.76	1.17
ON-OFF	0.52	1.38	0.90	0.26	1.96	4.83	2.64	6.04
ON-OFF	0.71	1.11	0.91	0.24	1.38	2.25	1.44	2.71
OFF-OFF	0.17	0.25	0.17	0.04	0.30	0.32	0.27	0.78
OFF-OFF	0.28	0.24	0.46	0.25	0.31	2.37	1.42	1.06
OFF-OFF	0.64	0.74	0.85	0.74	1.07	1.41	1.47	1.96
OFF-OFF	0.68	0.71	0.82	0.35	1.13	1.04	0.74	1.55
OFF-OFF	0.78	0.67	1.25	0.51	0.89	1.88	1.19	1.75
OFF-OFF	1.10	1.40	1.81	0.34	2.19	4.01	1.96	3.23

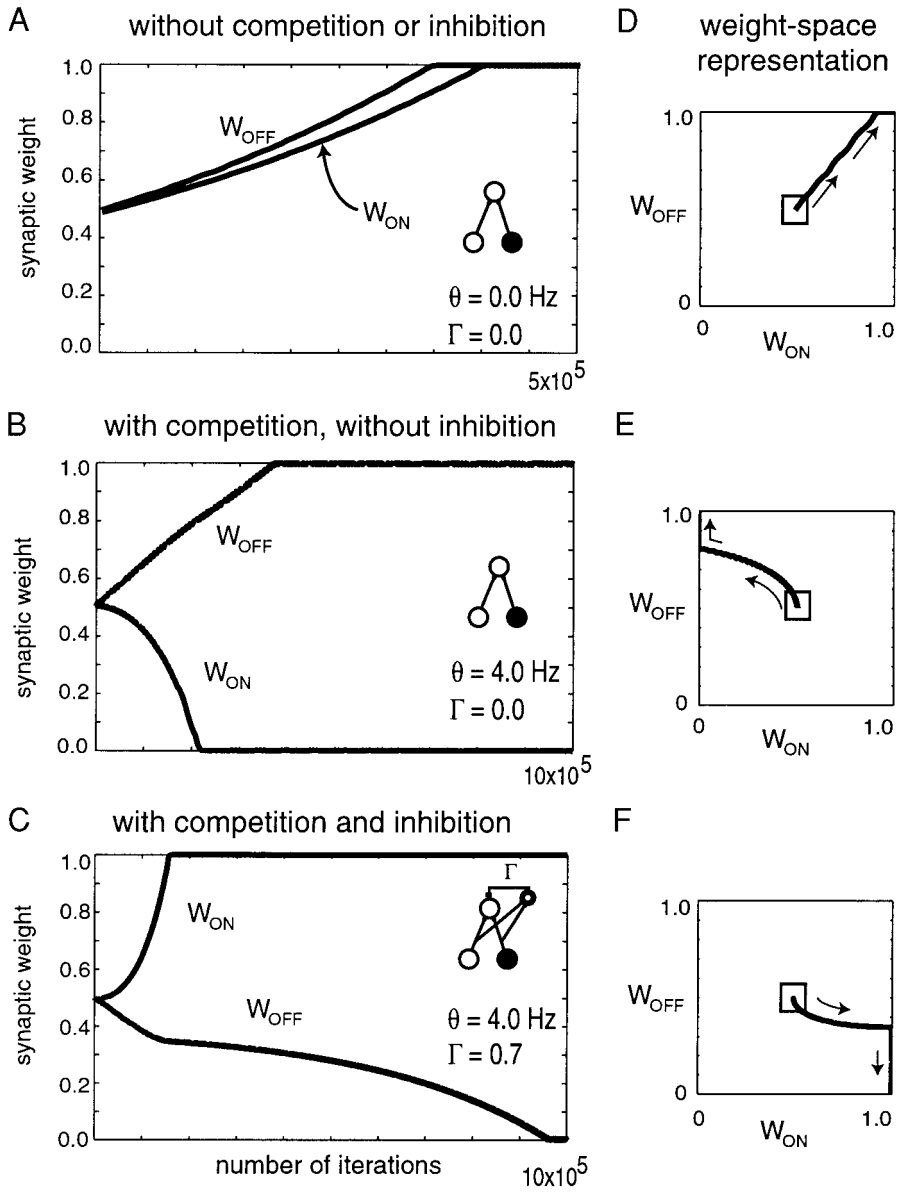

FIG. 5. Growth of synapses from initially converging RGC pairs. *A*: a typical example of the evolution of the synaptic strengths of an ON and an OFF pair over time without competition ($\theta = 0$ Hz) or inhibition ($\Gamma = 0$). The plot shows that with time ON and OFF synaptic weights (w_{ON} and w_{OFF}) increase, that is, both synapses grow together and no segregation occurs (initial strengths w_i chosen from a uniform random distribution in the range 0.45–0.55). *B*: plot of the evolution of the synaptic strengths of the same ON and OFF cell as in *A* but with competition added ($\theta = 4.0$ Hz) but no inhibition ($\Gamma = 0.0$). The weights now segregate with the OFF synapse strengthening to a maximum (1.0) and the ON synapse weakening to a minimum of 0.0. *C*: as in *B* but with inhibition added to the network ($\Gamma = 0.7$). The synapses again grow in opposite directions but now the ON synapse strengthens and the OFF synapse weakens. *D*: another representation of the data in *A* for synapses evolving without the competitive or inhibitory components of the network: The same simulation run as shown in *A* but represented as a "weight-space plot" that consists of a plot of w_{ON} vs. w_{OFF}. *E*: a re-graphing of the simulation data in *B* as a weight-space plot. The trajectory shown identifies the evolution of the system with competitive interactions between synapses but without inhibitory components. *F*: a re-graphing of the simulation data in *C* as a weight-space plot. The trajectory shown identifies the evolution of the system with both competitive and inhibitory components present.

general trends were supported in further simulations: it was found that for any pair it was possible to find these three types of behavior shown in Fig. 5, *A–C*, with a primitive form of ON-OFF segregation occurring when the synaptic weights of an ON-OFF pair grow in opposite directions.

As a tool for understanding solutions to our model, we also plot the development of w_1 versus w_2 in "weight-space." This weight-space representation of systems evolution allows us to summarize a large number of simulation runs as a series of trajectories through weight-space. When simulating networks starting with unbiased ON and OFF connections, the initial values of (w_{ON},w_{OFF}) are chosen at random from the interval [0.45,0.55] as indicated by the small squares in Fig. 5, *D–F*. The evolution over time of the synaptic weights is indicated by the trajectory of the line emerging out of the region of the initial conditions. Weight-space representations of the examples in Fig. 5, *A–C*, are shown to their right in Fig. 5, *D–F*, respectively. Observe that when the trajectory heads up and to the right, it indicates that the two synapses are growing together while if the trajectory heads either up and to the left corner or down and to the right corner the synapses are diverging.

Using the weight-space representation, we next present how synaptic weights of ON and OFF cells alter with time as a function of the main parameters in our model. The following subsections will examine: the role of θ; the role of Γ; and the degree to which ON-OFF activity differences drive segregation by quantifying the effect of the different ON-OFF input patterns.

EFFECTS OF θ ON SEGREGATION. For each value of θ, we chose a selection of initial weights and plotted their evolution as weight-space trajectories. Figure 6, *A–C*, illustrate the result when θ is varied while Γ is fixed at zero. For $\theta = 0$ Hz (Fig. 6*A*), any starting values of w_{ON} and w_{OFF} in weight-space are nearby a trajectory that sweeps up and to the right, indicating that the weights will always converge to their maximal strengths at the point (1,1). When θ increases to 3.9 Hz, the weight-space plot changes dramatically: there are now regions

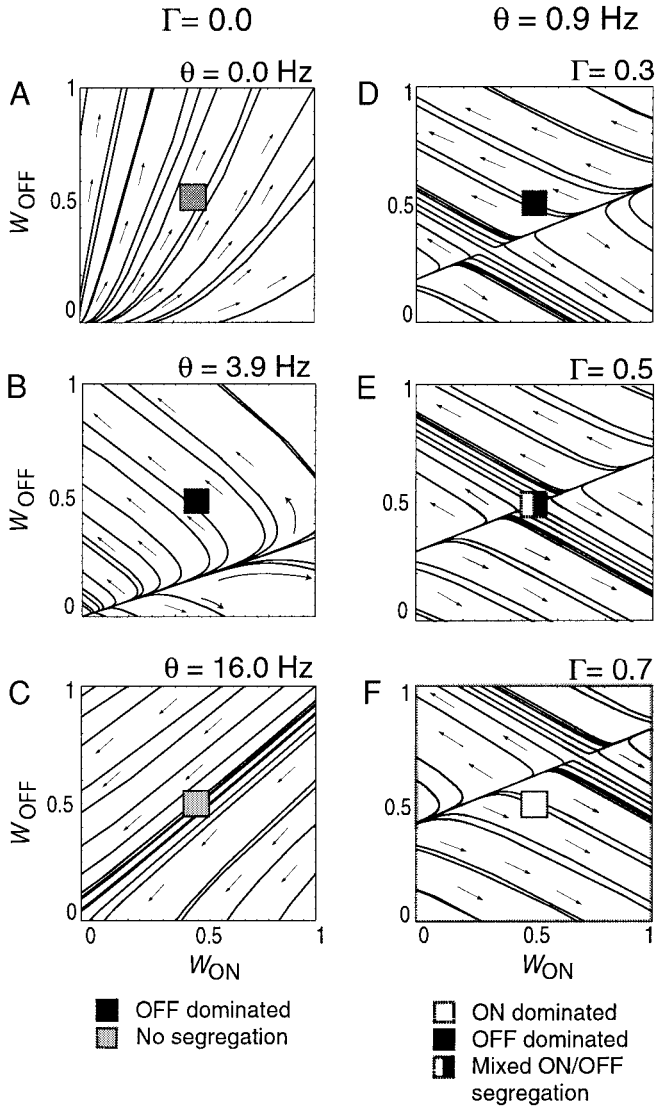

FIG. 6. Weight-space evolution as θ or Γ varies. (*A–C*) Behavior of weight-space plots obtained from representative ON and OFF pairs of cells as θ increases, for Γ fixed at 0. Other cell pairs produced similar results. Weight-space plots were obtained for a complete range of initial weights in [0,1]. By choosing any point within the square as an initial condition, one can then follow the evolution of the model from that point by interpolating a trajectory from the nearest flow lines. The shading of the squares indicates which sign dominated the square region corresponding to initial weights in the range [0.45,0.55]. Too little, θ = 0.0 Hz, or too much, θ=16.0 Hz, competition prevents segregation. (*D–F*) Weight-space plots as Γ varies from 0.3 to 0.7 while θ is fixed at 0.9 Hz. As Γ increases, a larger percentage of the weight-space corresponds to trajectories that result in ON cell inputs growing and OFF cell inputs decreasing.

of weight space that lead to different outcomes when the initial weights fall within them. The majority of the space leads to trajectories that sweep upward and to the left, with the OFF cell input winning over the ON cell. In contrast, there is a smaller region, roughly the region below the line that makes a 30° angle with the *x* axis, which will lead the weight trajectories sweeping to the right and downward. Thus the ON inputs win over the OFF inputs in this region of space. Finally, as θ becomes large (as compared with the input firing rates), all trajectories sweep down and to the left, with the minimum weight constraint on weights guiding the weights to converge on the origin. This implies that if competition is extremely intense, all synaptic connections will eventually be lost.

Γ DETERMINES THE PROBABILITY OF ON OR OFF CELL DOMINANCE AFTER SEGREGATION. The previous example illustrated the behavior of the system in the absence of an inhibitory component, i.e., for $\Gamma = 0$. Because inhibition can compensate for the OFF cells higher mean firing rates by inducing a compensating bias toward cells with lower firing rates, a nonzero Γ increases the probability of ON cells dominating rather than OFF cells. Figure 6, *D–F*, illustrates the effect of increasing Γ on the weight-space plots when θ is chosen to be sufficiently large to cause segregation. When Γ equals 0.5, the probability of ON or OFF cell winning are precisely equal, while for values of $\Gamma >$ 0.5, ON cells are more likely to win over OFF cells.

INPUTS FROM ON AND OFF CELL PAIRS ARE MORE LIKELY TO SEGREGATE COMPARED WITH ON AND ON, OR OFF AND OFF PAIRS. The preceding results show that for any cell pair, Hebbian rules can lead to the maintenance of one connection and the elimination of the other connection. However, the fundamental question here is whether different-signed pairs undergo elimination more easily than same-signed pairs. Figure 7 directly addresses this question by quantifying the (relative) probability of segregation for different pair types by treating θ as a random variable with a uniform distribution. For shorter time windows, ON-OFF pairs are significantly more likely to segregate than the like-signed ON-ON and OFF-OFF pairs. As the time window extends to 500 ms, the trend remains in place, but the differences narrow. Surprisingly, the ON-ON pairs are no longer significantly less likely to segregate than the ON-OFF pairs. Thus for Δt = 50 ms, it is clear that only the ON-OFF pairs compete for any substantial ranges of θ. These differences that come from changes in time windows raise the possibility that longer integration times favor convergence of nearby RGC afferents while shorter time scales may encourage segregation.

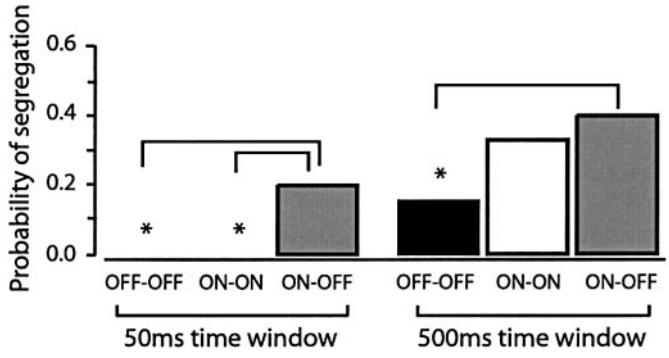

FIG. 7. The relative probability of segregation of cell pairs for the time windows Δt = 50 and 500 ms. For each cell pair type, 20 values of θ were chosen randomly from the uniform distribution [0,20] Hz. Γ was set to 0 because it influences only which cell will win but not the probability of segregation. For each value of θ, we used an eigenvector analysis to test whether segregation would occur. Same-signed pairs are less likely to segregate compared with opposite-signed pairs. *, a statistically significant (*t*-test: $P < 0.05$) difference as compared with the probability of segregation for the ON-OFF pairs at the same time scale. With its focus on a single parameter, θ, this technique should not be taken as a prediction of the overall probability of segregation occurring in the dLGN. Instead it allows us to compare the ease with which a value of θ can be found that will allow segregation to occur for different cell pair types.

Information from large populations of converging cells

RELATIONSHIP BETWEEN ACTION POTENTIALS AND CHANGES IN INTRACELLULAR CALCIUM. The spike recordings enabled us to study the temporal relationships of spiking of pairs of cells. However, immature dLGN neurons are known to receive connections from up to 20 RGCs during development (Chen and Regehr 2000). Therefore we would like to compare the temporal patterns of activity in larger populations of ON and OFF cells. This has previously been performed using calcium imaging, which also demonstrated that ON and OFF RGCs develop different calcium-activity patterns during ON-OFF segregation (Wong and Oakley 1996). To use these calcium recordings, we first asked whether the calcium changes correlate to spiking. We thus simultaneously recorded action potentials (cell-attached patch) and intracellular calcium levels in RGCs (data not shown). We found that each burst of action potentials correlated with a rise in intracellular calcium concentration in the cell body. A detectable calcium rise was observed even for one spike. The relative magnitude of each peak in calcium varied monotonically with the number of spikes, although it is not possible to resolve the temporal organization of the spikes within the burst. Our results thus show that calcium levels are closely related to changes in neuronal spike rates. Despite this, it is perhaps important to emphasize that calcium bursts represent a substantially different measure of retinal activity than the spiking rates used so far. In terms of our model, calcium bursts are a nonlinear measure of presynaptic spiking rates: one that trades off temporal resolution for a longer-lasting, more robust "all-or-none" signal.

MODELING RESULTS USING LARGE POPULATIONS OF RGCs. Having gained confidence that the calcium recordings report spike activity in the RGCs and that segregation of ON and OFF inputs can occur even at time windows >50 ms, we presented the patterns of activity reported by calcium levels to our model. In this next analysis, however, we also varied the number of cells initially connected to the postsynaptic dLGN cell. The input data came from six retinas, three from ages P9–11, and three from ages P16–22 (from Wong and Oakley 1996) (the number of ON and OFF cells were typically 8–10 cells of each type per retina). At P9–11, ON and OFF cells have similar spike patterns, in agreement with these calcium recordings (Myhr et al. 2001).

The calcium data were first converted to a binary signal indicating if the cell was bursting or silent (see Wong and Oakley 1996). This was a reasonable approximation and representation of the relative activity patterns of ON and OFF cells because their inputs to dLGN neurons can be potentiated or depressed only if bursts of action potentials, followed by long silent intervals, were evoked in the optic nerve (Mooney et al. 1993). A burst of spikes corresponded generally to a calcium peak. Our spike analysis suggests that segregation of ON and OFF inputs can occur even when spikes are integrated over time windows of up to (at least) 2 s (Fig. 4), which is more than sufficient to report the absence or presence of a calcium peak (each data point for the calcium measurements was the value averaged over 0.5 s time frames). Because each input cell's activity is 0 or 1, we just needed to test values for θ in the range 0–0.9 Hz; any value of $\theta > 1$ Hz would mean input activity was always below threshold. Values from 0–0.9 were selected for θ and Γ in increments of 0.1. From each retina, subsets of inputs from the ON and OFF classes were chosen and twenty simulations were run for each parameter combination. For each run, the degree of segregation (DSEG) and the ON-OFF bias were calculated (see METHODS). For each set of parameters, the average outcome of simulations based on the recorded populations of cells at both age groups were computed and displayed in Fig. 8. In Fig. 8, the radius (DSEG) is proportional to the extent of segregation, and the grayscale representation (SIGN) of each circle indicates whether ON or OFF populations dominated at the end of each simulation. Examples of the development of synaptic weights using representative inputs at different ages are shown in the accompanying movies. (Supplementary material may be viewed at http://jn.physiology.org/cgi/content/full/88/5/2311/DC1).

We first see that activity from P9–11 retinal inputs do not result in ON-OFF segregation (dots or very small circles), while for the same model parameters, inputs from P16–22 result in segregation (large circles, Fig. 8). This is true regardless of the

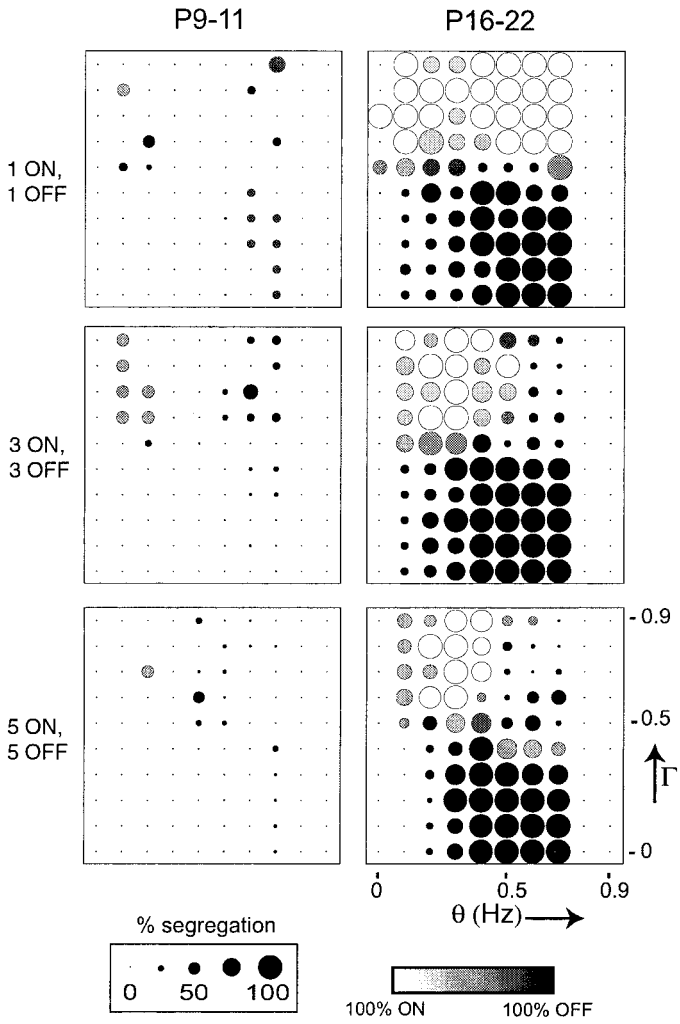

FIG. 8. Outcomes of synaptic competition between groups of ON and OFF cells. The input activity profiles of ON and OFF cells were obtained from prior calcium imaging studies (Wong and Oakley 1996). Each circle summarizes the results of 20 runs from different initial conditions (randomizing both the initial weights and the choice of retina and cells from which to take the calcium data) for a given value of θ and Γ. The circle radius is proportional to the mean value of *DSEG*; its color indicates the relative number of times the ON (white) or OFF (black) cell dominated (see scale bars).

number of inputs onto the dLGN cell. Second, we can see for the P16–22 retinas, the overall pattern of segregation is quite similar. ON cells tend to dominate for values of Γ above 0.5 and OFF cells tend to dominate for values of Γ below 0.5, while close to 0.5, there tends to be a split between ON and OFF domination. Third, we can see that, as expected, segregation always requires nonzero values of θ, but that a broad range of values for $\theta \in [0.2,0.5]$ Hz supports segregation as other parameters vary.

EFFECTS OF BIASED CONVERGENCE ON OUTCOMES. One mechanism that may aid in setting up ON and OFF sublaminae in the ferret is that initially cells in one layer receive more inputs from OFF RGCs while cells in the other layer receive more ON inputs. Differences in initial "input strength" may be due to differences in the relative number of ON and OFF cells contacting the dLGN neuron and/or differences in the synaptic weights of the initial connections from the cells. To test how such biased input configurations would influence Hebbian synaptic development, we performed simulations with different input configurations. Results of these simulations are shown in Fig. 9. From these simulations, it is clear that biases in inputs will tilt the outcome of the competition in favor of the initially dominant input.

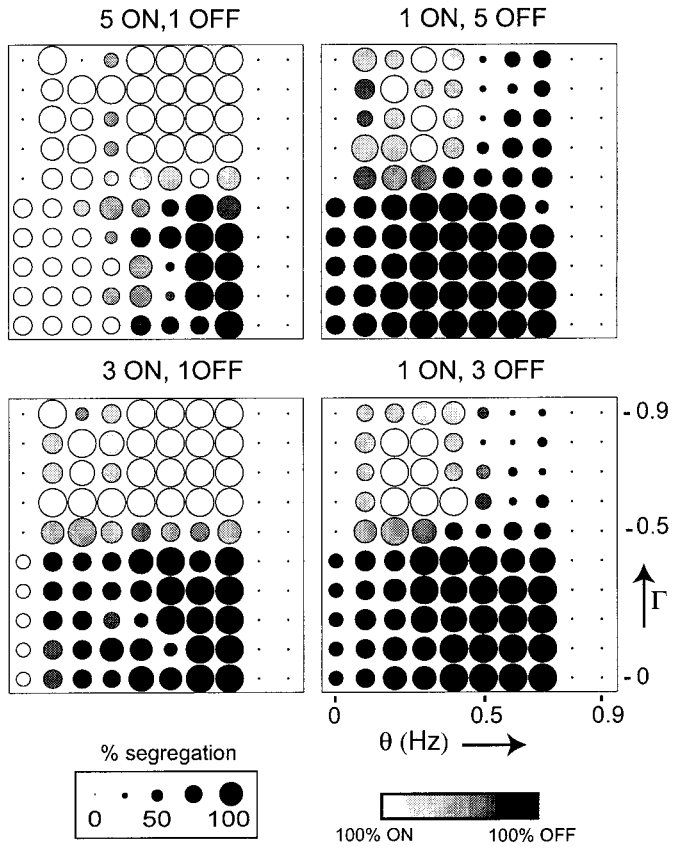

FIG. 9. Outcomes of initial biased convergence. The format is identical to that of Fig. 8. Unlike the previous simulations, when equal numbers of ON and OFF cells converged on a dLGN cell to form roughly equally strong connections, in these simulations the initial set of inputs is unbalanced. For example, the top left panel corresponds to cases in which there were 5 ON cell inputs and 1 OFF cell input. One can see that more parameter combinations lead to ON cell domination in this biased case than seen in the unbiased cases shown in Fig. 8 (P16–22). In general, the cell group which has initially more inputs is more likely to dominate the target cell at the end of the simulation.

DISCUSSION

We have shown with extracellular recordings that during the period of ON-OFF axonal segregation in the dLGN, ferret RGCs exhibit a firing pattern that distinguishes ON from OFF cells. Although ON and OFF RGCs show correlated rhythmic bursting activity, OFF RGCs spiked more frequently compared with ON cells. This resulted in a significant decrease in the degree of correlated spiking between the two populations of cells during the ON-OFF segregation period. The difference in firing patterns is due to changes in the intrinsic excitability and synaptic drives onto ON and OFF cells (Myhr et al. 2001). By presenting our recorded spike patterns to a linear Hebbian model, we found that differences in the activity patterns of ON and OFF cells are sufficient to cause segregation in their connectivity with geniculate neurons. Perhaps the most surprising aspect of our results may be that Hebbian mechanisms can lead to segregation of inputs from cells which fire synchronously. But, this result is intrinsic to the dynamical equations for Hebbian models such that in theory, one would predict that such systems can discriminate even between very small differences in group correlation. However, the results presented here are the first to demonstrate that this can happen in a biological system for which the endogenous pattern of presynaptic activity is known.

Factors influencing the outcome of ON and OFF retinogeniculate connectivity

Our results point out several aspects of how activity can determine the pattern of synaptic connectivity between the retina and the dLGN. First, competition between ON and OFF RGCs is necessary for segregation of their axonal projections. In the presence of competition, OFF cells generally outcompete ON cells when $\Gamma = 0$, i.e., in the absence of inhibitory influences. However, ON cells could succeed in gaining territory when inhibition was sufficiently large ($\Gamma \geq 0.5$). Although in the current model, we interpreted Γ in terms of the strength of a local inhibitory network, other mechanisms that reduce the competitive advantage of the more active cells can also be effective. It is interesting to note, however, that inhibition in the dLGN matures at the same time that ON-OFF segregation occurs in the dLGN (McCormick et al. 1995; Ramoa and McCormick 1994). We predict that maturation of the inhibitory network plays a role in shaping retinogeniculate connectivity by differentially affecting ON cells versus OFF cells. The importance of inhibition may be tested by pharmacologically modulating GABAergic activity in the dLGN.

A factor that appears to control how synaptic competition evolves concerns the time window for correlated pre- and postsynaptic activity (Bi and Poo 2001). Work in hippocampal and tectal neurons show that if inputs spike up to 20 ms before the postsynaptic cell spikes, those inputs are potentiated. Conversely, inputs that are activated 20 ms after the target cell fires are depressed. Because the overall time window within which spiking could strengthen or weaken synapses is around 40 ms, we examined the outcome of the competition between ON and OFF RGCs when this occurs within a time window of 50 ms.

Based on the recorded spike patterns, we observed a robust ability for dLGN cells to differentiate ON from OFF cells when a pair of these cells are connected to the dLGN cell (Fig. 7). ON and OFF inputs clearly segregate when spike timings are compared within 50 ms. But, at longer time scales (such as 500 ms), segregation is weaker for a pair of ON and OFF cells (Fig. 7). However, when larger numbers of cells were used as inputs (based on data from calcium imaging), ON-OFF segregation occurred whenever there was sufficient competition ($\theta > 0$ Hz). Our results suggest that most of the information that drives segregation may lie at shorter time scales but that segregation can still occur at longer time intervals, particularly for the calcium data.

We also asked under what conditions would an ON or an OFF cell win. Our simulations suggest that there are two major influencing factors. First, the level of inhibition determines whether an ON cell can outcompete an OFF cell. Second, inputs that initially are weighted in favor of one cell type could eventually help it to win, even if the firing rates of these cells are relatively lower. Such biases in connectivity might be set up by molecular cues that guide axon pathfinding into the dLGN so that cells initially receive dominant input from one RGC subtype. The initial convergence of ON and OFF inputs onto individual geniculate neurons remains to be determined. In sum, the synaptic inputs from ON cells could outcompete those of OFF cells when inhibition is relatively high (Fig. 8), and/or when their synaptic strengths start off much higher than that of OFF cells (Fig. 9).

Further modeling considerations

In our current model, the basic network comprises converging inputs from RGCs onto a geniculate neuron. A single RGC is likely to also connect to more than one geniculate neuron although how many is unknown. Thus elimination of one type of input onto a geniculate neuron also means that a presynaptic cell may lose connections to one target cell but maintain connections with another. Furthermore, while a postsynaptic cell may have limits as to how much "input" it can sustain (a limitation we considered in our model), the presynaptic cell may also have a constraint on how many synapses it can make and maintain. This concept of "resource allocation" has been formulated and explored in the neuromuscular junction (Barber and Lichtman 1999). At present, the lack of anatomical and physiological data concerning what type and where synapses are removed in the retinogeniculate pathway during the refinement process precludes examination of this concept in more detail.

We have also made a number of simple assumptions to facilitate analysis. Implicit in our model is the assumption that parameters such as θ and Γ remain fixed during the course of synaptic evolution. However, experimental results indicate that retinal activity varies greatly during development (Wong et al. 1993). For activity to guide synaptic refinement robustly, neurons need to be able to adapt to these changing levels of activity (Bear 1995; Golowasch et al. 1999; Turrigiano et al. 1995). One class of synaptic models deal with this problem by incorporating homeostatic mechanisms, which sense changing levels of activity and adjust parameters analogous to θ in response. For example, the BCM model (Bienenstock et al. 1982) uses a "sliding threshold" for activity that triggers synaptic enhancement versus weakening such that the threshold reflects changes in the overall level of input.

Our model also uses firing rates as its input activity. However, recent work (Bi and Poo 1998; Markram et al. 1997) has indicated that the timing of individual spikes in pre- and postsynaptic neurons may be important in synaptic modification. Also, theoretical analyses have shown that spike-timing-dependent Hebbian rules can adjust synaptic strengths with changing levels of input activity (Kempter et al. 1999; Song et al. 2000). A natural extension to the current work would be to include such timing-dependent effects into our model, especially if combined with simultaneous recordings from RGCs and dLGN cells (Kara et al. 2000). To further test whether segregation can occur at short (50 ms) and long (500 ms) time scales, spike recordings from identified populations of ON and OFF RGCs using a multielectrode array (Meister et al. 1991) will be necessary.

Why do ON and OFF cells maintain synchrony in their firing?

In a simplistic view, one would expect that inputs whose activities are completely asynchronous would segregate easily (Stent 1973). Why, then do ON and OFF cells maintain any level of synchrony in their firing? There are at least two possible reasons. First, eye-specific segregation has just occurred when ON-OFF segregation begins (Linden et al. 1981). Our analysis would suggest that the firing patterns of RGCs within an eye is likely to be more positively correlated compared with cells of the other eye, even during the period of ON-OFF segregation. This difference may help maintain the newly segregated afferents originating from the two eyes (Chapman 2000; Eglen 1999; Haith 1998) or from ON and OFF cells (Dubin et al. 1986). Second, retinal activity is also implicated in the refinement of retinotopic maps (Simon et al. 1992). The maps represent a systematic projection of neighboring RGCs to neighboring regions of their central targets. Because ON and OFF cells are located next to each other and waves still exist during the period of ON-OFF segregation, information about the relative locations of RGCs persists throughout the period of ON-OFF segregation. Thus it may be important that afferents from neighboring RGCs remain somewhat correlated for retinotopic maps to continue in their refinement.

Finally, further refinement in retinogeniculate connectivity occurs after ON and OFF inputs have initially segregated. This last phase of refinement involves a reduction of the number of same-sign RGCs connecting to an dLGN neuron (Chen and Regehr 2000; Tavazoie and Reid 2000), producing a sharpening of the receptive field of the dLGN neuron. As yet, we do not know if the spontaneous activity patterns of the ON and OFF cells could help drive this last phase of synaptic refinement. Our current recordings indicate that the spike patterns of cells within each ON or OFF subpopulation are not identical. However, because receptive field refinement occurs after eye opening, it remains possible that visual stimulation, rather than spontaneous activity, shapes receptive field refinement of geniculate neurons, as demonstrated for RGCs (Sernagor and Grzywacz 1996). How spontaneous and visually evoked activity act together to further sculpt or maintain connections in the visual system remains a challenging issue to pursue.

We thank the members of the Wong laboratory and Dr. Charlie Anderson for insightful discussions and critical reading of the manuscript.

This work was supported by the National Institutes of Health (R.O.L. Wong) and a Wellcome Trust International Fellowship (S. J. Eglen).

REFERENCES

ANDERSON E, SORENSEN D, BISCHOF C, DONGARRA J, DEMMEL J, HAMMARLING S, BAI Z, CROZ JD, GREENBAUM A, MCKENNEY A, AND OSTROUCH S. *LAPACK User's Guide*. Society for Industrial and Applied Mathematics, Philadelphia, 1995.

BARBER MU AND LICHTMAN JW. Activity-driven synapse elimination leads paradoxically to domination by inactive neurons. *J Neurosci* 19: 9975–9985, 1999.

BEAR MF. Mechanism for a sliding synaptic modification threshold. *Neuron* 15: 1–4, 1995.

BI G AND POO MM. Synaptic modifications in cultured hippocampal neurons: dependence on spike timing, synaptic strength, and postsynaptic cell type. *J Neurosci* 18: 10464–10472, 1998.

BI G AND POO MM. Synaptic modification by correlated activity: Hebb's postulate revisited. *Annu Rev Neurosci* 24: 139–166, 2001.

BIENENSTOCK EL, COOPER LN, AND MUNRO PW. Theory for the development of neuron selectivity: orientation specificity and binocular interaction in visual cortex. *J Neurosci* 2: 32–48, 1982.

BODNARENKO SR, YEUNG G, THOMAS L, AND MCCARTHY M. The development of retinal ganglion cell dendritic stratification in ferrets. *Neuroreport* 10: 2955–2959, 1999.

CHAPMAN B. Necessity for afferent activity to maintain eye-specific segregation in ferret lateral geniculate nucleus. *Science* 287: 2479–2482, 2000.

CHEN C AND REGEHR WG. Developmental remodeling of the retinogeniculate synapse. *Neuron* 28: 955–966, 2000.

CRAMER KS AND SUR M. Blockade of afferent impulse activity disrupts on/off sublamination in the ferret lateral geniculate nucleus. *Brain Res Dev Brain Res* 98: 287–290, 1997.

DUBIN MW, STARK LA, AND ARCHER SM. A role for action-potential activity in the development of neuronal connections in the kitten retinogeniculate pathway. *J Neurosci* 6: 1021–1036, 1986.

EGLEN SJ. The role of retinal waves and synaptic normalization in retinogeniculate development. *Philos Trans R Soc Lond B Biol Sci* 354: 497–506, 1999.

GOLOWASCH J, CASEY M, ABBOTT LF, AND MARDER E. Network stability from activity-dependent regulation of neuronal conductances. *Neural Comput* 11: 1079–1096, 1999.

GOODHILL GJ AND LÖWEL S. Theory meets experiment—correlated neural activity helps determine ocular dominance column periodicity. *Trends Neurosci* 18: 437–439, 1995.

GOODMAN CS AND SHATZ CJ. Developmental mechanisms that generate precise patterns of neuronal connectivity. *Cell* 72 *Suppl*: 77–98, 1993.

HAHM JO, LANGDON RB, AND SUR M. Disruption of retinogeniculate afferent segregation by antagonists to NMDA receptors. *Nature* 351: 568–570, 1991.

HAITH GL. *Modeling Activity-Dependent Development in the Retinogeniculate Projection* (PhD thesis). Stanford, CA: Stanford University, 1998.

HEBB D. *The Organization of Behaviour*. New York: Wiley, 1949.

HERTZ J, KROGH A, AND PALMER RG. *Introduction to the Theory of Neural Computation*. Redwood City, CA: Addison-Wesley, 1991.

KARA P, REINAGEL P, AND REID RC. Low response variability in simultaneously recorded retinal, thalamic, and cortical neurons. *Neuron* 27: 635–646, 2000.

KEMPTER R, GERSTNER W, AND VAN HEMMEN JL. Hebbian learning and spiking neurons. *Phys Rev E* 59: 4498–4514, 1999.

KOCH C AND SEGEV I (Editors). *Methods in Neuronal Modeling* (2nd ed.). Cambridge, MA: MIT Press, 1998.

LEWICKI MS. A review of methods for spike sorting: the detection and classification of neural action potentials. *Network* 9: R53–R78, 1998.

LINDEN DC, GUILLERY RW, AND CUCCHIARO J. The dorsal lateral geniculate-nucleus of the normal ferret and its postnatal-development. *J Comp Neurol* 203: 189–211, 1981.

LINSKER R. From basic network principles to neural architecture. *Proc Natl Acad Sci USA* 83: 7508–7512, 1986.

LINSKER R. Self-organization in a perceptual network. *Computer* 21: 105–117, 1988.

LOHMANN C AND WONG ROL. Cell-type specific dendritic contacts between retinal ganglion cells during development. *J Neurobiol* 48: 150–162, 2001.

MACKAY DJC AND MILLER KD. Analysis of Linsker's simulations of hebbian rules. *Neural Comput* 2: 173–187, 1990.

MARKRAM H, LUBKE J, FROTSCHER M, AND SAKMANN B. Regulation of synaptic efficacy by coincidence of postsynaptic APs and EPSPs. *Science* 275: 213–215, 1997.

MCCORMICK DA, TRENT F, AND RAMOA AS. Postnatal development of synchronized network oscillations in the ferret dorsal lateral geniculate and perigeniculate nuclei. *J Neurosci* 15: 5739–5752, 1995.

MEISTER M, WONG ROL, BAYLOR DA, AND SHATZ CJ. Synchronous bursts of action potentials in ganglion cells of the developing mammalian retina. *Science* 252: 939–943, 1991.

MILLER KD. Derivation of linear hebbian equations from a nonlinear hebbian model of synaptic plasticity. *Neural Comput* 2: 321–333, 1990.

MILLER KD. Models of activity-dependent neural development. *Prog Brain Res* 102: 303–318, 1994.

MILLER KD. Synaptic economics: competition and cooperation in synaptic plasticity. *Neuron* 17: 371–374, 1996.

MILLER KD, KELLER JB, AND STRYKER MP. Ocular dominance column development: analysis and simulation. *Science* 245: 605–615, 1989.

MOONEY R, MADISON DV, AND SHATZ CJ. Enhancement of transmission at the developing retinogeniculate synapse. *Neuron* 10: 815–825, 1993.

MYHR KL, LUKASIEWICZ PD, AND WONG ROL. Mechanisms underlying developmental changes in the firing patterns of on and off retinal ganglion cells during refinement of their central projections. *J Neurosci* 21: 8664–8671, 2001.

RAMOA AS AND MCCORMICK DA. Developmental changes in electrophysiological properties of LGNd neurons during reorganization of retinogeniculate connections. *J Neurosci* 14: 2089–2097, 1994.

SANES JR AND LICHTMAN JW. Development of the vertebrate neuromuscular junction. *Annu Rev Neurosci* 22: 389–442, 1999.

SERNAGOR E AND GRZYWACZ NM. Influence of spontaneous activity and visual experience on developing retinal receptive fields. *Curr Biol* 6: 1503–1508, 1996.

SIMON DK, PRUSKY GT, O'LEARY DDM, AND CONSTANTINE-PATON M. N-methyl-d-aspartate receptor antagonists disrupt the formation of a mammalian neural map. *Proc Natl Acad Sci USA* 89: 10593–10597, 1992.

SONG S, MILLER KD, AND ABBOTT LF. Competitive Hebbian learning through spike-timing-dependent synaptic plasticity. *Nat Neurosci* 3: 919–926, 2000.

STENT G. A physiological mechanism for Hebb's postulate of learning. *Proc Natl Acad Sci USA* 70: 997–1001, 1973.

STRYKER MP AND STRICKLAND SL. Physiological segregation of ocular dominance columns depends on the pattern of afferent electrical activity. *Invest Opthalmol Vis Sci* 25 *Suppl*: 278, 1984.

TAVAZOIE SF AND REID RC. Diverse receptive fields in the lateral geniculate nucleus during thalamocortical development. *Nat Neurosci* 3: 608–616, 2000.

TURRIGIANO G, LEMASSON G, AND MARDER E. Selective regulation of current densities underlies spontaneous changes in the activity of cultured neurons. *J Neurosci* 15: 3640–3652, 1995.

VAN OOYEN A. Competition in the development of nerve connections: a review of models. *Network* 12: R1–R47, 2001.

WÄSSLE H AND BOYCOTT BB. Functional architecture of the mammalian retina. *Physiol Rev* 71: 447–480, 1991.

WOLFRAM S. *The Mathematica Book*. Cambridge, UK: Cambridge Univ. Press, 1999.

WONG ROL. Retinal waves and visual system development. *Annu Rev Neurosci* 22: 29–47, 1999.

WONG ROL, MEISTER M, AND SHATZ CJ. Transient period of correlated bursting activity during development of the mammalian retina. *Neuron* 11: 923–938, 1993.

WONG ROL AND OAKLEY DM. Changing patterns of spontaneous bursting activity of on and off retinal ganglion cells during development. *Neuron* 16: 1087–1095, 1996.

ZAHS KR AND STRYKER MP. Segregation of ON and OFF afferents to ferret visual cortex. *J Neurophysiol* 59: 1410–1429, 1988.